Acta Pharmacologica Sinica

ARTICLE

IMM-H007 attenuates isoprenaline-induced cardiac fibrosis through targeting TGFβ1 signaling pathway

Shuai-xing Wang[1], Ye-nan Feng[1], Shan Feng[1], Ji-min Wu[1], Mi Zhang[1], Wen-li Xu[1], You-yi Zhang[1], Hai-bo Zhu[2], Han Xiao[1] and Er-dan Dong[1]

Upon chronic stress, β-adrenergic receptor activation induces cardiac fibrosis and leads to heart failure. The small molecule compound IMM-H007 has demonstrated protective effects in cardiovascular diseases via activation of AMP-activated protein kinase (AMPK). This study aimed to investigate IMM-H007 effects on cardiac fibrosis induced by β-adrenergic receptor activation. Because adenosine analogs also exert AMPK-independent effects, we assessed AMPK-dependent and -independent IMM-H007 effects in murine models of cardiac fibrosis. Continual subcutaneous injection of isoprenaline for 7 days caused cardiac fibrosis and cardiac dysfunction in mice in vivo. IMM-H007 attenuated isoprenaline-induced cardiac fibrosis, diastolic dysfunction, α-smooth muscle actin expression, and collagen I deposition in both wild-type and AMPKα2$^{-/-}$ mice. Moreover, IMM-H007 inhibited transforming growth factor β1 (TGFβ1) expression in wild-type, but not AMPKα2$^{-/-}$ mice. By contrast, IMM-H007 inhibited Smad2/3 signaling downstream of TGFβ1 in both wild-type and AMPKα2$^{-/-}$ mice. Surface plasmon resonance and molecular docking experiments showed that IMM-H007 directly interacts with TGFβ1, inhibits its binding to TGFβ type II receptors, and downregulates the Smad2/3 signaling pathway downstream of TGFβ1. These findings suggest that IMM-H007 inhibits isoprenaline-induced cardiac fibrosis via both AMPKα2-dependent and -independent mechanisms. IMM-H007 may be useful as a novel TGFβ1 antagonist.

Keywords: IMM-H007; sympathetic stress; cardiac fibrosis; AMP-activated protein kinase; transforming growth factor β1

Acta Pharmacologica Sinica (2022) 43:2542–2549; https://doi.org/10.1038/s41401-022-00899-2

INTRODUCTION

Cardiac fibrosis, which is characterized by a net accumulation of extracellular matrix (ECM) in the myocardium [1, 2], is an integral component of most cardiac pathologic conditions and eventually leads to heart failure [3]. Besides the renin-angiotensin-aldosterone system [4], chronic catecholamine stimulation of adrenoceptors has been proven to induce cardiac fibrosis [5, 6]. Finding new effective therapeutic drugs for myocardial fibrosis and heart failure caused by different etiologies is an important issue in clinical practice. The adenosine compound IMM-H007 (also called WS070117, patent number WO/2010/040286) showed improved oral bioavailability in vivo compared to the traditional adenosine analog AICAR [7, 8]. IMM-H007 has demonstrated protective effects in cardiovascular diseases via activation of the adenosine 5′-monophosphate (AMP)-activated protein kinase (AMPK) [9]. IMM-H007 alleviates atherosclerosis by inhibiting endothelial inflammation and promoting activation of the endothelial nitric oxide synthase to improve endothelial dysfunction [10–12]. However, the role of IMM-H007 in chronic β-adrenergic stimulation-induced cardiac fibrosis and the involved mechanisms have not been comprehensively elucidated and require further studies.

In addition to AMPK activation, adenosine analogs also have AMPK-independent effects. It has been reported that the adenosine analog AICAR decreases glucose phosphorylation [13] and gluconeogenesis [14] in an AMPK-independent manner. Whether IMM-H007 also exerts AMPK-independent effects remains to be elucidated.

In the present study, we investigated the effects of IMM-H007 on cardiac fibrosis induced by chronic β-adrenergic stimulation, determined whether AMPK-independent pathways participate in the protective effects of IMM-H007, and identified the involved mechanisms.

MATERIALS AND METHODS

Antibodies and reagents

IMM-H007 was synthesized in the Department of Medicinal Chemistry, Institute of Materia Medica, Chinese Academy of Medical Sciences and Peking Union Medical College. Antibodies against Smad2/3, phospho-Smad2 (Ser465/467)/Smad3 (Ser423/425), AMPKα, phospho-AMPKα (Thr172), and GAPDH were obtained from Cell Signaling Technology (Beverly, MA, USA). AMPKα2, α-smooth muscle actin (α-SMA), and collagen type I antibodies were obtained from Abcam (Cambridge, UK).

[1]Department of Cardiology and Institute of Vascular Medicine, Peking University Third Hospital, NHC Key Laboratory of Cardiovascular Molecular Biology and Regulatory Peptides, Key Laboratory of Molecular Cardiovascular Science, Ministry of Education, Beijing Key Laboratory of Cardiovascular Receptors Research, Beijing 100191, China and [2]State Key Laboratory for Bioactive Substances and Functions of Natural Medicines, Beijing Key Laboratory of New Drug Mechanisms and Pharmacological Evaluation Study, Institute of Materia Medica, Chinese Academy of Medical Sciences and Peking Union Medical College, Beijing 100050, China
Correspondence: Hai-bo Zhu (zhuhaibo@imm.ac.cn) or Han Xiao (xiaohan@bjmu.edu.cn)

Received: 13 January 2022 Accepted: 7 March 2022
Published online: 30 March 2022

Animals

All experimental protocols involving animals were approved by the Committee of Peking University on the Ethics of Animal Experiments (LA2016-018). The study was conducted in accordance with the Use of Laboratory Animals published by the US National Institutes of Health (NIH Publication No. 85-23, revised 2011) and the guidelines of the Peking University Health Science Centre. Homozygous AMPKα2$^{-/-}$ mice on C57BL/6 background were kindly provided by Dr. Benoit Viollet (Institute National de la Santé et de la Recherche Médicale U567, Paris). Male AMPKα2$^{-/-}$ mice and wild-type (WT) littermates were kept in a specific pathogen-free environment (temperature: 20–24 °C; relative humidity: 30%–70%) on a 12:12 h light:dark cycle and received standard rodent food.

WT ($n = 24$) and AMPKα2 knockout ($n = 24$) animals were randomly divided into four experimental groups: vehicle ($n = 6$), IMM-H007 ($n = 6$), isoprenaline (ISO) ($n = 6$), and IMM-H007 + ISO ($n = 6$). None of the animals were excluded from the analysis. Three days before the ISO treatment, daily treatment with IMM-H007 (200 mg·kg^{-1}·day^{-1} body weight, ig) or normal solvent (sodium carboxymethyl cellulose) was initiated and was continued until 7 days after ISO treatment (10 mg·kg^{-1}·day^{-1} body weight, sc). After continual ISO injection for 7 days, the mice were euthanized by an ip injection with an overdose of sodium pentobarbital. Cardiac samples were collected in lysis buffer (10 mmol·L^{-1} Tris-HCl, pH 7.4; 100 mmol·L^{-1} NaCl; 1 mmol·L^{-1} EDTA; 1 mmol·L^{-1} EGTA; 1 mmol·L^{-1} NaF; 20 mmol·L^{-1} $Na_4P_2O_7$; 2 mmol·L^{-1} Na_3VO_4; 1% Triton X-100; 10% glycerol; 0.1% sodium dodecyl sulfate (SDS); 1% deoxycholic acid; 1 mmol·L^{-1} PMSF; and 1 g·mL^{-1} aprotinin).

Isolation and culture of primary mouse cardiac fibroblasts

Mouse cardiac fibroblasts (CFs) were prepared from the hearts of 6–8-week-old C57BL/6 mice as described previously [15]. Heart tissues were excised, cut into 1–2-mm^3 pieces, and digested with collagenase type II (300U·mL^{-1}, Gibco, Carlsbad, CA, USA). Dissociated cells were plated into 100-mm culture dishes in Dulbecco's Modified Eagle's Medium with 10% fetal bovine serum and incubated for 48 h. The medium was changed every other day. Cells were kept at 37 °C in a humidified 5% CO_2 environment. Isolated CFs (0 passages) were seeded at a density of 15,000 cells/cm^2. At 80%–90% confluence, cells were passaged using standard trypsinization techniques. Cells in the first passage were used for the further cell experiments.

Histochemical staining

Murine hearts were removed, washed with cold phosphate-buffered saline, fixed with 4% paraformaldehyde for 8 h, and embedded in paraffin. Serial sections (5 μm thick) were stained with picrosirius red to detect collagen deposition as described previously [16]. Tissue morphometry was evaluated in a blinded fashion using a Leica Q550 IW imaging workstation (Leica Microsystems Imaging Solutions Ltd., Cambridge, UK). The fibrotic area (red color) was expressed as a percentage of the total area using computer-assisted image analysis software (Image-Pro Plus, version 6.0, Media Cybernetics Corporation, Rockville, MD, USA).

Hydroxyproline assay

Hydroxyproline content was measured using a hydroxyproline assay kit (Jiancheng Bioengineering Institute, Nanjing, China). The results were expressed as micrograms per milligram of tissue wet weight.

Echocardiography

Echocardiography was used to evaluate cardiac function after ISO administration as previously described [16]. We used a VisualSonics high-resolution Vevo 2100 system (VisualSonics Inc., Toronto, Canada). In brief, the mice were anesthetized with 1.0% isoflurane until the heart rate was stabilized at 350–400 bpm. An apical four-chamber view was acquired, and the peak flow velocities during early diastole (E wave) were measured across the mitral valve. Early diastolic peak velocity (E' wave) of the mitral valve ring was also measured in this view, and the ratio E/E' was calculated to assess left ventricular diastolic function.

Enzyme-linked immunosorbent assay (ELISA)

Transforming growth factor β1 (TGFβ1) protein levels in the hearts were measured using an ELISA kit (R&D Systems Incorporated, Minneapolis, MN, USA). The procedures were conducted according to the manufacturer's instructions, and the absorbances were measured at 450 and 570 nm with a Multiskan GO instrument (Thermo Fisher Scientific Cellomics, Pittsburgh, PA, USA). All values were in the linear range and were calculated based on known protein concentrations. Final results were expressed as picograms per milligram of total protein.

Western blot analysis

The levels of Smad2/3, phospho-Smad2 (Ser465/467)/Smad3 (Ser423/425), AMPKα, phospho-AMPKα (Thr172), AMPKα2, α-SMA, collagen type I, and GAPDH were examined using Western blotting. Total proteins were extracted with RIPA buffer (6.5 mmol·L^{-1} Tris, pH 7.4, 15 mmol·L^{-1} NaCl, 1 mmol·L^{-1} EDTA, 0.1% SDS, 0.25% sodium deoxycholate, 1% NP-40). Protein concentrations were measured with bicinchoninic acid reagents, and 30–60 μg of protein samples were separated by 10% sodium dodecyl sulfate-polyacrylamide gel electrophoresis and transferred to nitrocellulose membranes. The blots were immunoreacted with primary antibodies for at least 8 h at 4 °C. After the membranes had been incubated with the corresponding horseradish peroxidase (HRP)-conjugated secondary antibodies (ZSGB-BIO, Beijing, China), protein bands were visualized with a chemiluminescent HRP substrate (Millipore Corporation, kit No. WBKLS0500), and blot images were obtained using a Syngene GeneGnome-XRQ-NPC imager (Gene Company, Shanghai, China). The protein levels were quantified by calculating the greyscale value of each band using ImageJ (version 1.43, National Institutes of Health, Bethesda, MD, USA) software.

Molecular docking and molecular dynamics simulation

The ligand IMM-H007 was processed in the LigPrep module in Schrödinger 10.2 software (Schrödinger, LLC, NY, USA). The OPLS3 force field was adopted to perform energy minimization. The crystal structure of TGFβ1 was retrieved from the RCSB Protein Data Bank. The crystallographic structure of 3KFD was prepared using the Protein Preparation Wizard module. Glide was applied to predict the potential binding mode of IMM-H007 with the TGFβ1 protein. Following the docking results, independent 30-ns molecular dynamics simulations were performed using Desmond. Na^+ and Cl^- ions were each added at the physiological concentration of 0.15 mol·L^{-1} to ensure the overall neutrality of the systems. Simulations were conducted with an OPLS3 force field and a TIP3P explicit solvent model. The final size of the solvated system was close to ~24,000 atoms. A 5-ps recording interval was chosen, and the NPT ensemble was employed with a fixed temperature of 300 K and pressure of 1.01 bar. The analysis tool of the Simulation Interactions Diagram was used to monitor ligand-protein interactions.

Surface plasmon resonance (SPR) spectroscopy

Experiments were performed at 25 °C using a Biacore T200, and the data were analyzed using Biacore T200 evaluation software 2.0 (GE Healthcare, Stockholm, Sweden). TGFβ1 was covalently coupled to a CM5 chip (GE Healthcare), and IMM-H007 was injected in a two-fold dilution concentration series ranging from 6.25 μmol·L^{-1} to 0.19 μmol·L^{-1}. Steady-state values were calculated from sensorgrams and plotted against concentrations. Data were fitted to a single-site binding model to calculate the K_D value.

For competition experiments, buffer scouting using the A-B-A mode of the Biacore 8 K method wizard was selected to evaluate the effects of IMM-H007 on TGFβ binding affinity toward the extracellular ligand-binding domain of the TGFβ type II receptor. TGFβ type II

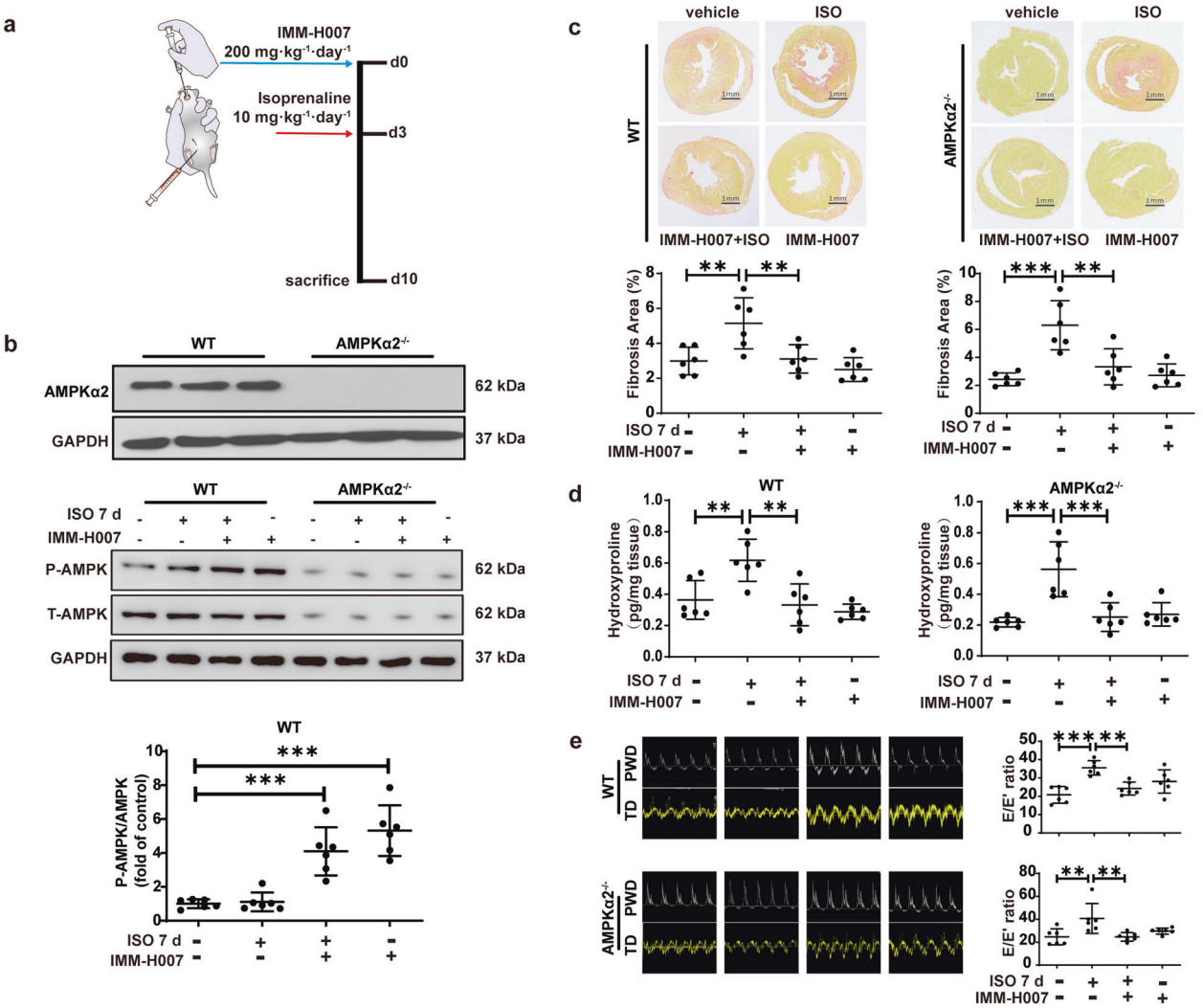

Fig. 1 IMM-H007 inhibits ISO-induced fibrosis and diastolic dysfunction independent of AMPKα2 expression. a IMM-H007 (200 mg·kg^{-1}·day^{-1} body weight) was given once per day for 10 days through oral gavage. ISO (10 mg·kg^{-1}·day^{-1} body weight, sc) was administered once per day for 7 days. **b** Western blots to measure phosphorylated AMPK, total AMPK, and AMPKα2 expression in WT and AMPKα2$^{-/-}$ mice. **c** Representative micrographs of picrosirius red-stained sections of the heart in WT and AMPKα2$^{-/-}$ mice (scale bars: 1 mm). The mean cardiac interstitial collagen in picrosirius red-stained sections is expressed as the percent collagen (lower panels). **d** Collagen concentration in the heart as determined by hydroxyproline assays in WT and AMPKα2$^{-/-}$ mice. **e** Representative images of PWD sonography showing the mitral flow, TD sonography of the mitral valve ring, and E/E' values on the period of 7 days of the ISO treatment in WT and AMPKα2$^{-/-}$ mice. $n = 6$; $^{**}P < 0.01$; $^{***}P < 0.001$. One-way ANOVA with Tukey's post hoc test. AMPK AMP-activated protein kinase, IMM IMM-H007, ISO isoprenaline, PWD pulsed-wave Doppler, TD tissue Doppler, WT wild-type.

receptors (R&D Systems Incorporated, Minneapolis, MN, USA) were immobilized on a CM5 sensor chip by using standard amine-coupling at 25 °C with running HEPES-P buffer (20 mM HEPES buffer, 2.7 mM NaCl, 137 mM KCl, 0.05% surfactant P20, pH 7.4). A reference channel was only activated and blocked to eliminate unspecific compound binding to the surface of the chip. The immobilization level of the TGFβ type II receptor was about 1000 RU. TGFβ1 at a concentration of 1 nmol·L^{-1} and the mixture of TGFβ1 (1 nmol·L^{-1}) and IMM-H007 (6 μmol·L^{-1}) were serially injected into the channel to evaluate the binding affinity. Extra wash steps with 50% DMSO were added to remove the last remaining sample in the pipeline.

Statistical analysis

Data are expressed as means ± standard deviations. All samples were independent. For parametric analyses, the data were normally distributed and were tested for homogeneity of variance. Data with more than two groups were analyzed using the one-way ANOVA with a two-sided Tukey's *post hoc* test. The data were analyzed using GraphPad Prism software (version 8.43, GraphPad Software Inc., San Diego, CA, USA). A P value < 0.05 was considered statistically significant.

RESULTS

IMM-H007 inhibits ISO-induced fibrosis and diastolic dysfunction independently of AMPKα2 effects

IMM-H007 is a small molecule compound that can activate AMPK. First, we detected the expression and phosphorylation of AMPK in both WT and AMPKα2$^{-/-}$ mice. IMM-H007 significantly increased AMPK phosphorylation in WT mice but not in AMPKα2$^{-/-}$ mice (Fig. 1a, b). Because overactivation of β-adrenergic receptors can lead to cardiac inflammation and fibrosis, we used the nonselective β-adrenergic receptor agonist ISO to simulate cardiac fibrosis induced by sympathetic hyperactivation. As expected, the results of picrosirius red stainings showed that IMM-H007 significantly decreased the ISO-induced increase in fibrotic area. The results of

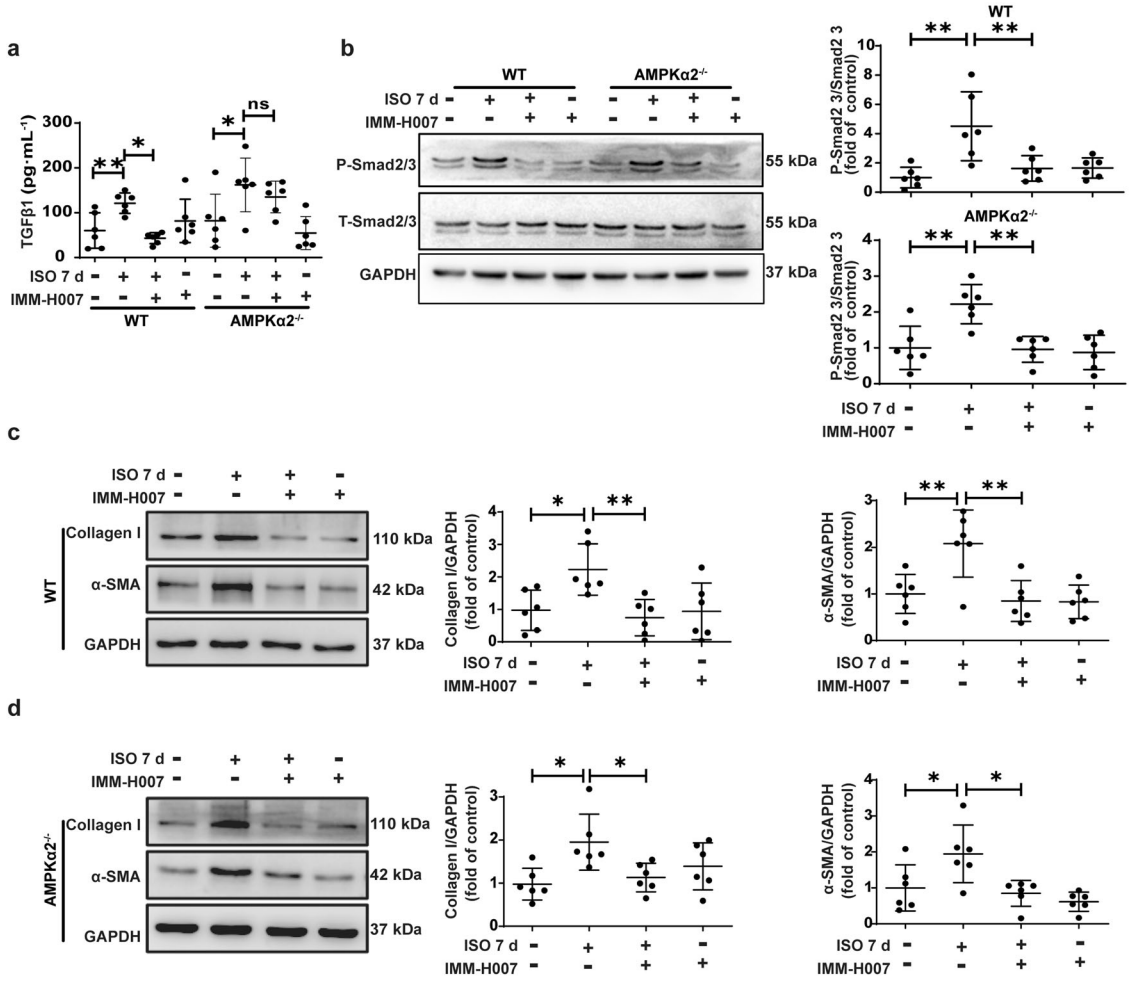

Fig. 2 IMM-H007 reduces ISO-induced Smad2/3 phosphorylation downstream of TGFβ1 and cardiac fibrosis via an AMPKα2-independent pathway, but the inhibition of TGFβ1 expression is in an AMPKα2-dependent manner. a TGFβ1 protein levels as determined by ELISAs. **b** Representative Western blots of phosphorylated Smad2/3 in WT and AMPKα2$^{-/-}$ mice. **c** Western blot analysis to quantify collagen I and α-SMA in the hearts of WT mice. **d** Protein levels of collagen I and α-SMA in the hearts of AMPKα2$^{-/-}$ mice. $n = 6$; $^{*}P < 0.05$; $^{**}P < 0.01$. One-way ANOVA with Tukey's *post hoc* test. α-SMA α-smooth muscle actin, AMPK AMP-activated protein kinase, IMM IMM-H007, ISO isoprenaline, TGFβ1 transforming growth factor β1, WT wild-type.

the hydroxyproline assay suggested that ISO-induced collagen deposition was significantly decreased by IMM-H007 (Fig. 1c). To further investigate whether AMPK is essential for IMM-H007 inhibition of cardiac fibrosis, we treated WT and AMPKα2$^{-/-}$ mice with IMM-H007 (200 mg·kg^{-1}·day^{-1}) or normal saline. Similar to observations in WT mice, IMM-H007 significantly reduced in AMPKα2$^{-/-}$ mice the area of fibrosis induced by ISO treatment. Hydroxyproline expression was significantly increased after ISO treatment but was significantly decreased after pretreatment with IMM-H007 in both WT and AMPKα2$^{-/-}$ mice (Fig. 1d). Cardiac diastolic dysfunction after ISO treatment was also alleviated by IMM-H007 pretreatment. As shown by echocardiography, IMM-H007 significantly inhibited ISO-induced diastolic dysfunction not only in WT mice but also in AMPKα2$^{-/-}$ mice (Fig. 1e).

These results demonstrated that IMM-H007 inhibits ISO-induced cardiac fibrosis and diastolic dysfunction independently of AMPKα2 expression.

IMM-H007 reduces ISO-induced Smad2/3 phosphorylation downstream of TGFβ1 and cardiac fibrosis via an AMPKα2-independent pathway, but the inhibition of TGFβ1 expression is AMPKα2-dependent

TGFβ1 plays a key role in the development of cardiac fibrosis. To investigate the mechanism involved in the attenuation of ISO-induced cardiac fibrosis by IMM-H007 treatment, we measured the expression of TGFβ1 using ELISAs. In vivo, TGFβ1 protein expression was increased in ISO-treated mice compared to the vehicle group, and IMM-H007 treatment inhibited this ISO-induced TGFβ1 upregulation in WT mice. By contrast, IMM-H007 did not affect ISO-induced TGFβ1 expression in AMPKα2$^{-/-}$ mice (Fig. 2a). We then investigated TGFβ1 downstream signaling. TGFβ1-Smad2/3 signaling is a major pathway involved in myofibroblast activation and ECM deposition. Western blotting demonstrated that IMM-H007 pretreatment significantly inhibited ISO-induced Smad2/3 phosphorylation not only in WT mice but also in AMPKα2$^{-/-}$ mice (Fig. 2b).

In the process of cardiac fibrosis, collagen I is a major ECM constituent in ISO-induced cardiac fibrosis. The expression levels of collagen I protein were measured by Western blotting. In WT mice, collagen I was upregulated in the ISO group but was significantly decreased in the ISO group with IMM-H007 pretreatment. α-SMA is a marker of activated myofibroblasts, which secrete ECM proteins. As shown by Western blotting, α-SMA expression was markedly increased after ISO treatment but was significantly decreased by prior IMM-H007 administration (Fig. 2c). However, in contrast to the TGFβ1 results, Western blots of samples from AMPKα2$^{-/-}$ mice demonstrated that ISO-induced

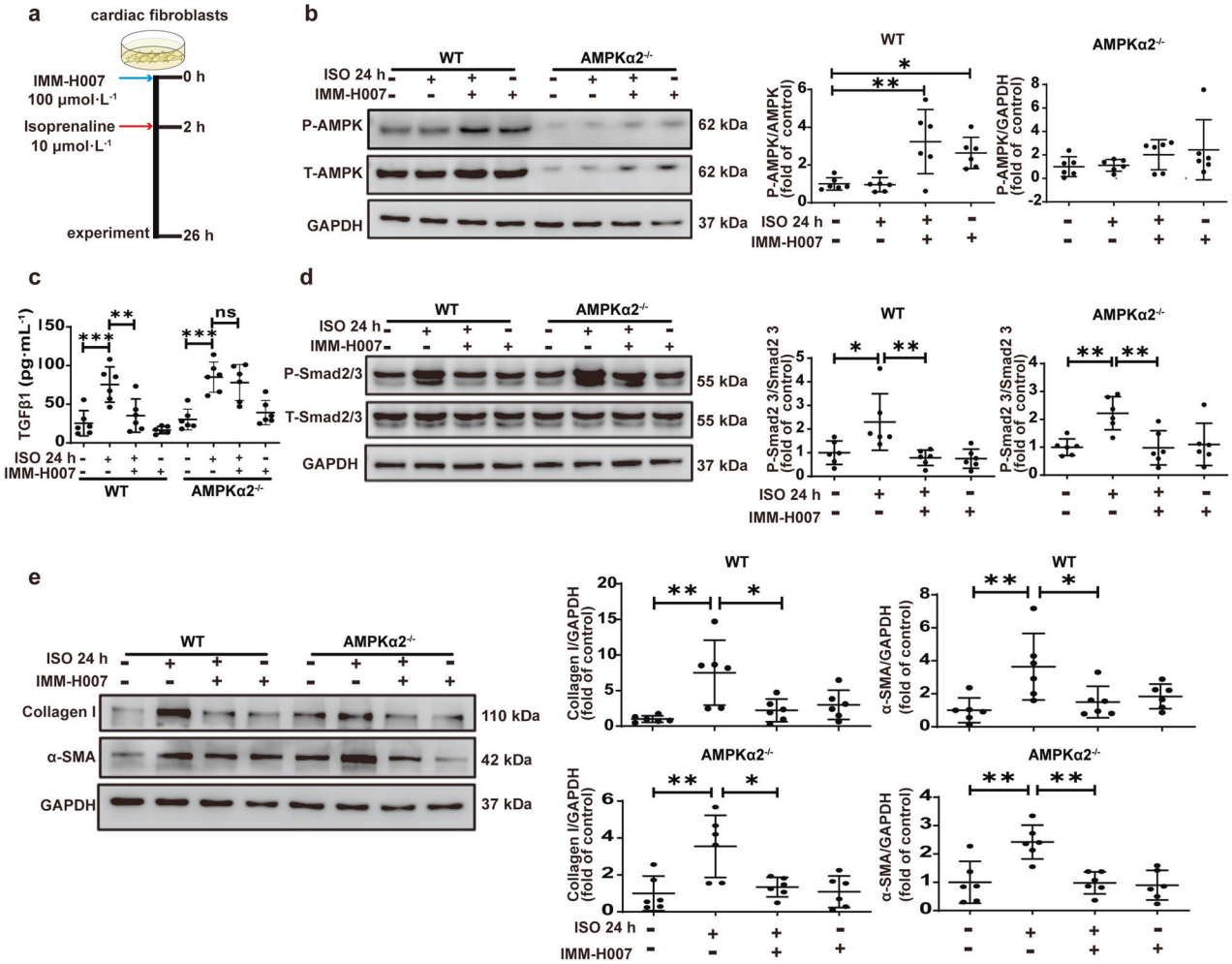

Fig. 3 In cardiac fibroblasts, IMM-H007 inhibits TGFβ1 expression via AMPKα2, but inhibition of Smad2/3 signaling downstream of TGFβ1 is independent of AMPKα2. a CFs were treated with ISO (10 μmol·L^{-1}) for 24 h following IMM-H007 (100 μmol·L^{-1}) pretreatment for 2 h. **b** Representative Western blots of phosphorylated AMPK in WT and AMPKα2$^{-/-}$ CFs. **c** TGFβ1 protein levels in CFs as determined by ELISAs. **d** Representative Western blots of phosphorylated Smad2/3 in WT and AMPKα2$^{-/-}$ CFs. **e** Western blot analysis of collagen I and α-SMA expression in CFs. $n = 6$; *$P < 0.05$; **$P < 0.01$; ***$P < 0.001$. One-way ANOVA with Tukey's post hoc test. AMPK AMP-activated protein kinase, CF cardiac fibroblast, IMM IMM-H007, ISO isoprenaline, TGFβ1 transforming growth factor β1, WT wild-type.

collagen I and α-SMA expression levels were also significantly decreased after IMM-H007 pretreatment (Fig. 2d).

These results suggested that IMM-H007 inhibits ISO-induced TGFβ1 expression in an AMPKα2-dependent manner, but the inhibition of the Smad2/3 signaling pathway downstream of TGFβ1 and the reduction of collagen I and α-SMA expression are independent of AMPKα2.

In CFs, IMM-H007 inhibition of TGFβ1 expression depends on AMPKα2, but the inhibition of the Smad2/3 signaling pathway downstream of TGFβ1 is AMPKα2-independent

To further define the mechanism for the attenuation of ISO-induced cardiac fibrosis by treatment with IMM-H007, we isolated primary CFs from adult WT and AMPKα2$^{-/-}$ mice. Similar to the findings in vivo, IMM-H007 significantly increased AMPK phosphorylation in WT, but not AMPKα2$^{-/-}$, CFs in vitro (Fig. 3a, b). ELISA results showed that IMM-H007 inhibited ISO-induced TGFβ1 expression in WT CFs but not in AMPKα2$^{-/-}$ CFs (Fig. 3c). These data suggest that the inhibitory effect of IMM-H007 on ISO-induced TGFβ1 expression was dependent on AMPKα2.

In cultured CFs from adult mice, Western blotting showed that IMM-H007 significantly reduced ISO-induced Smad2/3 phosphorylation in both WT and AMPKα2$^{-/-}$ CFs (Fig. 3d), which was similar to the results of in vivo experiments. Western blotting showed that collagen I and α-SMA expression levels were significantly increased after ISO treatment but were significantly decreased after IMM-H007 pretreatment of CFs in both WT and AMPKα2$^{-/-}$ mice (Fig. 3e).

Together, these results indicated that IMM-H007 attenuates ISO-induced phosphorylation of Smad2/3 independent of the AMPKα2 pathway. Furthermore, IMM-H007 reduced ISO-induced α-SMA expression and collagen I deposition in CFs independently of AMPKα2 activation.

IMM-H007 antagonizes TGFβ1 signal transduction through direct interaction with TGFβ1

In AMPKα2$^{-/-}$ mice and CFs, IMM-H007 inhibited TGFβ downstream signal transduction but did not reduce TGFβ1 expression. This suggested that IMM-H007 may interact directly with TGFβ1. To further explore the observed IMM-H007 effects, docking studies and molecular dynamics simulations were performed. It was found that IMM-H007 engaged in several interactions with TGFβ1 (Fig. 4a). The aromatic rings of IMM-H007 were situated in a cave-like structure consisting of the β-strand1 and β-strand2, forming hydrogen bonds with Arg 25 and Ile 33, respectively. The purine skeleton also formed an aromatic stack with His 34.

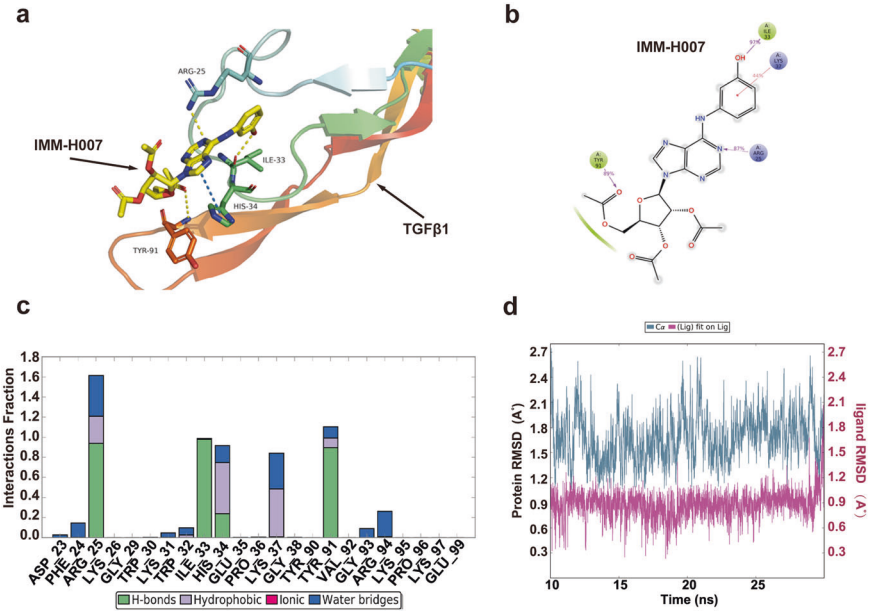

Fig. 4 IMM-H007 antagonizes TGFβ1 signal transduction through direct interaction with TGFβ1. a Predicted binding mode of IMM-H007 with TGFβ1 (PDB id: 3KFD). **b**, **c** Protein-ligand contact histogram of IMM-H007 and the corresponding 2D diagram predicted through MD simulations. A percentage value suggests that for X% of the simulation time, the specific interaction is maintained. **d** RMSD of TGFβ1 interaction with the ligand IMM-H007 in MD simulations. MD molecular dynamics, RMSD root mean square deviation, TGFβ1 transforming growth factor β1.

Besides, the relative flexible tetrahydrofuran ring extended to the solvent area, forming another hydrogen bond with Tyr 91.

As shown in the protein-ligand contact histogram, the results were consistent with those of the docking study (Fig. 4b, c). Two hydrogen bonds formed by the purine core with Arg 25 and Ile 33 were maintained during 87% and 97% of the simulation time, respectively. Arg 25 also participated in water bridges and hydrophobic interaction, which contributed to the ligand-binding affinity. The hydrophilic side chain of the tetrahydrofuran ring formed another hydrogen bond with Tyr 91 occupying 89% of the simulation time. The purine skeleton was well embedded in the binding pocket, forming a cation-Π stack with His 34. To verify the binding mode of IMM-H007 in a dynamic condition, a 30-ns molecular dynamic simulation was performed using Desmond. The complex was stable after 10-ns simulations (Fig. 4d), and the last 20-ns trajectories were extracted and analyzed. Overall, these findings provide guidance to better understand the IMM-H007 mechanisms and may facilitate the search for optimized TGFβ1 inhibitors in the future.

IMM-H007 directly interacts with TGFβ1, inhibits its binding to the TGFβ receptor, and attenuates TGFβ1 downstream signaling

To verify whether IMM-H007 can directly bind to TGFβ1, we conducted SPR experiments. The findings of the SPR-based assay suggested that the binding of IMM-H007 to TGFβ1 occurred with a K_D value of 0.2098 μmol·L^{-1} (Fig. 5a). Next, we premixed TGFβ1 with IMM-H007 for 2 h. The SPR-based assay showed that IMM-H007 reduced the binding between TGFβ1 and its receptor, the TGFβ type II receptor (Fig. 5b). Consistent with these results, Western blotting analyses indicated that IMM-H007 decreased TGFβ1-induced phosphorylation of Smad2/3 (Fig. 5c, d). These results suggested that IMM-H007 interacts directly with TGFβ1, inhibits TGFβ1 binding to its receptor, and attenuates its downstream Smad2/3 signaling.

DISCUSSION

In the present study, we demonstrated that IMM-H007 inhibits β-adrenergic stimulation-induced cardiac fibrosis through both AMPKα2-dependent and -independent pathways. IMM-H007 reduces TGFβ1 expression in an AMPK-dependent manner. By contrast, IMM-H007 inhibits ISO-induced Smad2/3 phosphorylation, a signal downstream of TGFβ1, independent of AMPKα2 activation. Furthermore, we found that IMM-H007 directly binds to TGFβ1, inhibits TGFβ1 ligand binding to its receptor, and reduces its downstream signaling (Fig. 6).

It is generally accepted that IMM-H007 has protective effects by activating AMPK. IMM-H007 has been reported to promote angiogenesis and reduce atherosclerosis via AMPK activation [11]. AMPK activation has been shown to reduce cardiac fibrosis by inhibiting TGFβ1 expression [17, 18] and activating peroxisome proliferator-activated receptor α [19]. It has also been reported that IMM-H007 can reduce angiotensin II-induced TGFβ1 expression and cardiac fibrosis, in which AMPKα is also activated [20]. In the present study, AMPKα2 deficiency blocked the inhibitory effect of IMM-H007 on ISO-induced TGFβ1 expression, suggesting that the IMM-H007-induced inhibition of TGFβ1 expression is AMPK-dependent. However, in our study, AMPKα2 deficiency only partially blocked the inhibitory effect of IMM-H007 on cardiac fibrosis, suggesting that IMM-H007 protects against cardiac fibrosis by additional mechanisms other than AMPK activation.

AMPK agonists such as AICAR and metformin have been reported to act in an AMPK-independent manner [13, 14, 21, 22]. In the present study, we also found that IMM-H007 attenuated cardiac fibrosis by targeting Smad2/3 phosphorylation downstream of TGFβ1 in both WT and AMPKα2 knockout mice. Thus, targeting Smad2/3 signaling independently of AMPKα2 may be partially responsible for the protective effects of IMM-H007 against cardiac fibrosis, suggesting that IMM-H007 also exerts AMPK-independent effects.

The AMPK-independent effect of IMM-H007 observed in this study was similar to that of metformin, another well-known AMPK agonist. Several studies have reported that metformin acts via AMPK-independent pathways [23, 24], and our previous study found that metformin inhibits TGFβ1 downstream signaling by binding to TGFβ1 [21]. In the present study, we found that IMM-H007 also can bind to TGFβ1. The TGFβ1 binding regions to

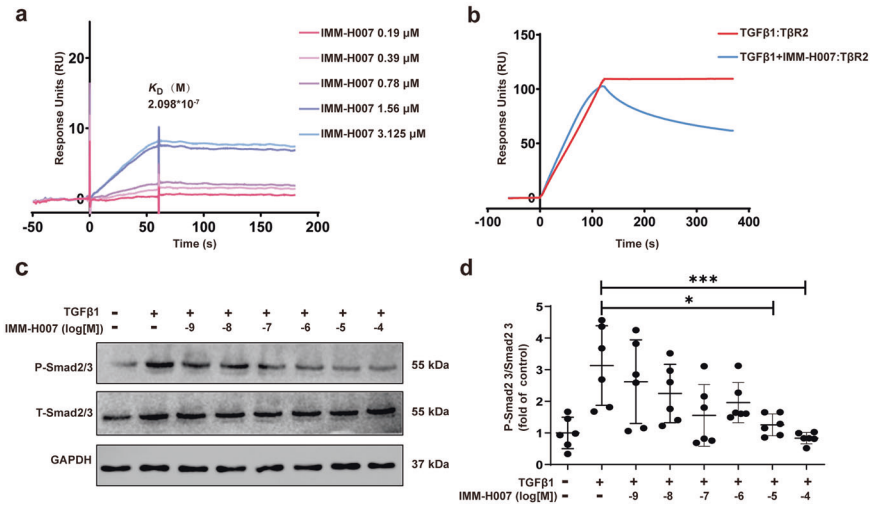

Fig. 5 IMM-H007 directly interacts with TGFβ1, inhibits binding to its receptor, and attenuates its downstream signaling. a SPR analysis of the binding between IMM-H007 and TGFβ1. Recombinant TGFβ1 protein was immobilized on an activated CM5 sensor chip, and IMM-H007 was then flowed across the chip. **b** Overlay plots of SPR sensorgrams depicting the binding of IMM-H007 to TGFβ1 and the inhibitory effect on binding between TGFβ1 and TβR2 (IMM-H007 concentration: 6 μmol·L^{-1}). **c**, **d** IMM-H007 and TGFβ1 (0.5 ng·mL^{-1}) were premixed for 2 h, and CFs were subsequently treated with this mixture for 24 h. Western blot analysis and quantification of phosphorylated Smad2/3, Smad2/3, and GAPDH were performed. $n = 6$; $^{*}P < 0.05$; $^{***}P < 0.001$. One-way ANOVA with Tukey's post hoc test. SPR surface plasmon resonance, TGFβ1 transforming growth factor β1, TβR2 transforming growth factor β1 receptor II, IMM IMM-H007, CF cardiac fibroblast.

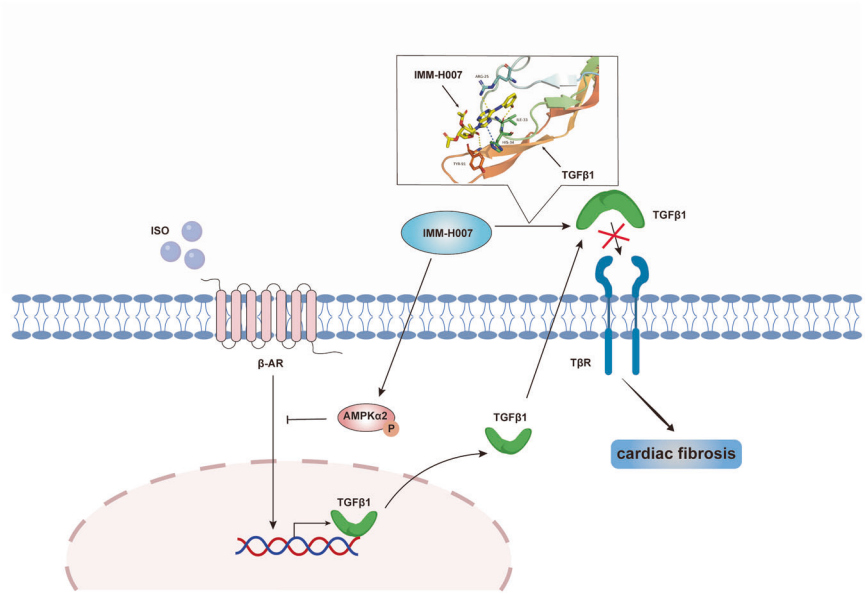

Fig. 6 Schematic showing how IMM-H007 alleviates ISO-induced cardiac fibrosis via AMPK-dependent and -independent pathways. IMM IMM-H007, ISO isoprenaline, AMPK AMP-activated protein kinase, TGFβ1 transforming growth factor β1, TβR TGFβ1 receptor.

IMM-H007 and metformin are both located near Arg 25, which is also the region where TGFβ1 binds to its receptor.

It is also possible that the protective effects of IMM-H007 observed in AMPKα2$^{-/-}$ mice might be caused by the activation of other AMPKα isoforms. AMPKα has two isoforms in heart but AMPKα1/AMPKα2 double-knockout causes lethality of embryos. Since AMPKα2 is the dominant isoform in the heart [25], the knockout of this subtype is used in the present study. As shown in Fig. 1b, AMPKα2 deficiency dramatically inhibit the phosphorylation of AMPK in the heart following IMM-H007 treatment. The phosphorylation level is comparable to, if not lower than, the base level in untreated mice. However, the inhibition of AMPK activation failed to inhibit the anti-fibrosis effect of IMM-H007, which indicates that IMM-H007 can bind to additional targets other than AMPK. Indeed, we further prove that IMM-H007 can directly bind and inhibit TGFβ1. Nevertheless, we strongly agree that AMPKα1 may also be involved in the protective effect of IMM-H007 in AMPKα2-deficient mice, as it is compensatory to AMPKα2 [26] and plays cardioprotective roles in cardiac remodeling [27, 28].

TGFβ1 is involved in many diseases, especially tumors and fibrosis. TGFβ1 induces liver [29] and kidney [30] fibrosis, and it can also induce epithelial-mesenchymal transition, which plays a key role in carcinoma progression and organ fibrosis [31, 32]. Thus, targeting the TGFβ1 signaling pathway has become attractive for drug development. The present study demonstrated that IMM-H007 had a higher affinity to TGFβ1 than metformin [21]. Our study identified IMM-H007 as a novel TGFβ1 suppressor, and this action underlies the pleiotropic effects of this drug. This finding

provides new indications for IMM-H007, including numerous TGFβ1-associated diseases. IMM-H007 is a small molecule compound that can easily reach the targeted tissue not only in the heart, but also in other organs, and has the potential to bind TGFβ1 in other organs or disease models. Based on the interaction between IMM-H007 and TGFβ1, new compounds targeting TGFβ1 can be developed based on IMM-H007 with similar characteristics but higher specificity and potency.

In conclusion, we demonstrated that IMM-H007 attenuates cardiac fibrosis via both AMPKα2-dependent and -independent pathways. The underlying mechanisms include IMM-H007 targeting of TGFβ1 production in an AMPKα2-dependent manner and IMM-H007 binding to TGFβ1 and targeting of Smad2/3 signaling downstream of TGFβ1 in an AMPKα2-independent manner. We found that IMM-H007 is a novel TGFβ1 inhibitor, providing a possible approach to treat a variety of TGFβ1-related diseases besides cardiac fibrosis.

ACKNOWLEDGEMENTS

This work was supported by the National Key R&D Program (grant numbers 2020YFC2004704 to HX), Natural Science Foundation of China (grant numbers 82030072 to HX, 81830009 to YYZ, and 82070235 to EDD), the Beijing Municipal Natural Science Foundation (grant number 7191013 to EDD), Research Unit of Medical Science Research Management/Basic and Clinical Research of Metabolic Cardiovascular Diseases, Chinese Academy of Medical Sciences (2021RU003 to EDD), and the Key Clinical Projects of Peking University Third Hospital [BYSYZD2019022 to HX].

AUTHOR CONTRIBUTIONS

HX, EDD, YYZ, and HBZ conceived the project and designed the study. HBZ provided the drug. SXW, YNF, SF, and MZ performed the experiments. SXW, JMW, and WLX analyzed the data. SXW, JMW, and YNF wrote the manuscript.

ADDITIONAL INFORMATION

Competing interests: The authors declare no competing interests.

REFERENCES

1. Travers JG, Kamal FA, Robbins J, Yutzey KE, Blaxall BC. Cardiac fibrosis: the fibroblast awakens. Circ Res. 2016;118:1021–40.
2. Kong P, Christia P, Frangogiannis NG. The pathogenesis of cardiac fibrosis. Cell Mol Life Sci. 2014;71:549–74.
3. Berk BC, Fujiwara K, Lehoux S. ECM remodeling in hypertensive heart disease. J Clin Invest. 2007;117:568–75.
4. Weber KT, Sun Y, Bhattacharya SK, Ahokas RA, Gerling IC. Myofibroblast-mediated mechanisms of pathological remodelling of the heart. Nat Rev Cardiol. 2013;10:15–26.
5. Fu Y, Xiao H, Zhang Y. Beta-adrenoceptor signaling pathways mediate cardiac pathological remodeling. Front Biosci (Elite Ed). 2012;4:1625–37.
6. Anand IS, Fisher LD, Chiang YT, Latini R, Masson S, Maggioni AP, et al. Changes in brain natriuretic peptide and norepinephrine over time and mortality and morbidity in the Valsartan Heart Failure Trial (Val-HeFT). Circulation. 2003;107:1278–83.
7. Dixon R, Gourzis J, McDermott D, Fujitaki J, Dewland P, Gruber H. AICA-riboside: safety, tolerance, and pharmacokinetics of a novel adenosine-regulating agent. J Clin Pharmacol. 1991;31:342–7.
8. Sun Y, Lian Z, Jiang C, Wang Y, Zhu H. Beneficial metabolic effects of 2′,3′,5′-triacetyl-N_6-(3-hydroxylaniline) adenosine in the liver and plasma of hyperlipidemic hamsters. PLoS One. 2012;7:e32115.
9. Lian Z, Li Y, Gao J, Qu K, Li J, Hao L, et al. A novel AMPK activator, WS070117, improves lipid metabolism discords in hamsters and HepG2 cells. Lipids Health Dis. 2011;10:67.
10. Huang L, Fan B, Ma A, Shaul PW, Zhu H. Inhibition of ABCA1 protein degradation promotes HDL cholesterol efflux capacity and RCT and reduces atherosclerosis in mice. J Lipid Res. 2015;56:986–97.
11. Chen B, Li J, Zhu H. AMP-activated protein kinase attenuates oxLDL uptake in macrophages through PP2A/NF-κB/LOX-1 pathway. Vasc Pharmacol. 2016;85:1–10.
12. Wang MJ, Peng XY, Lian ZQ, Zhu HB. The cordycepin derivative IMM-H007 improves endothelial dysfunction by suppressing vascular inflammation and promoting AMPK-dependent eNOS activation in high-fat diet-fed ApoE knockout mice. Eur J Pharmacol. 2019;852:167–78.
13. Guigas B, Bertrand L, Taleux N, Foretz M, Wiernsperger N, Vertommen D, et al. 5-Aminoimidazole-4-carboxamide-1-β-D-ribofuranoside and metformin inhibit hepatic glucose phosphorylation by an AMP-activated protein kinase-independent effect on glucokinase translocation. Diabetes. 2006;55:865–74.
14. Foretz M, Hébrard S, Leclerc J, Zarrinpashneh E, Soty M, Mithieux G, et al. Metformin inhibits hepatic gluconeogenesis in mice independently of the LKB1/AMPK pathway via a decrease in hepatic energy state. J Clin Invest. 2010;120:2355–69.
15. Mia MM, Cibi DM, Ghani SA, Singh A, Tee N, Sivakumar V, et al. Loss of *Yap/Taz* in cardiac fibroblasts attenuates adverse remodeling and improves cardiac function. Cardiovasc Res. 2021. https://doi.org/10.1093/cvr/cvab205.
16. Xiao H, Li H, Wang JJ, Zhang JS, Shen J, An XB, et al. IL-18 cleavage triggers cardiac inflammation and fibrosis upon β-adrenergic insult. Eur Heart J. 2018;39:60–9.
17. Wu D, Lei H, Wang JY, Zhang CL, Feng H, Fu FY, et al. CTRP3 attenuates post-infarct cardiac fibrosis by targeting Smad3 activation and inhibiting myofibroblast differentiation. J Mol Med. 2015;93:1311–25.
18. Mishra R, Cool BL, Laderoute KR, Foretz M, Viollet B, Simonson MS. AMP-activated protein kinase inhibits transforming growth factor-β-induced Smad3-dependent transcription and myofibroblast transdifferentiation. J Biol Chem. 2008;283:10461–9.
19. Fujita K, Maeda N, Sonoda M, Ohashi K, Hibuse T, Nishizawa H, et al. Adiponectin protects against angiotensin II-induced cardiac fibrosis through activation of PPAR-α. Arterioscler Thromb Vasc Biol. 2008;28:863–70.
20. Ge W, Zhang W, Gao R, Li B, Zhu H, Wang J. IMM-H007 improves heart function via reducing cardiac fibrosis. Eur J Pharmacol. 2019;857:172442.
21. Xiao H, Zhang J, Xu Z, Feng Y, Zhang M, Liu J, et al. Metformin is a novel suppressor for transforming growth factor (TGF)-β1. Sci Rep. 2016;6:28597.
22. Feng Y, Wang S, Zhang Y, Xiao H. Metformin attenuates renal fibrosis in both AMPKα2-dependent and independent manners. Clin Exp Pharmacol Physiol. 2017;44:648–55.
23. Xiao H, Ma X, Feng W, Fu Y, Lu Z, Xu M, et al. Metformin attenuates cardiac fibrosis by inhibiting the $TGFβ_1$–Smad3 signalling pathway. Cardiovasc Res. 2010;87:504–13.
24. Lin CC, Yeh HH, Huang WL, Yan JJ, Lai WW, Su WP, et al. Metformin enhances cisplatin cytotoxicity by suppressing signal transducer and activator of transcription-3 activity independently of the liver kinase B1-AMP-activated protein kinase pathway. Am J Respir Cell Mol Biol. 2013;49:241–50.
25. Stapleton D, Mitchelhill KI, Gao G, Widmer J, Michell BJ, Teh T, et al. Mammalian AMP-activated protein kinase subfamily. J Biol Chem. 1996;271:611–4.
26. Qiu S, Liu T, Piao C, Wang Y, Wang K, Zhou Y, et al. AMPKα2 knockout enhances tumour inflammation through exacerbated liver injury and energy deprivation-associated AMPKα1 activation. J Cell Mol Med. 2019;23:1687–97.
27. Noppe G, Dufeys C, Buchlin P, Marquet N, Castanares-Zapatero D, Balteau M, et al. Reduced scar maturation and contractility lead to exaggerated left ventricular dilation after myocardial infarction in mice lacking AMPKα1. J Mol Cell Cardiol. 2014;74:32–43.
28. Dufeys C, Daskalopoulos EP, Castanares-Zapatero D, Conway SJ, Ginion A, Bouzin C, et al. AMPKα1 deletion in myofibroblasts exacerbates post-myocardial infarction fibrosis by a connexin 43 mechanism. Basic Res Cardiol. 2021;116:10.
29. Duvnjak M, Tomasic V, Gomercic M, Smircic Duvnjak L, Barsic N, Lerotic I. Therapy of nonalcoholic fatty liver disease: current status. J Physiol Pharmacol. 2009;60:57–66.
30. Bottinger EP, Bitzer M. TGF-β signaling in renal disease. J Am Soc Nephrol. 2002;13:2600–10.
31. Chapman HA. Epithelial-mesenchymal interactions in pulmonary fibrosis. Annu Rev Physiol. 2011;73:413–35.
32. Derynck R, Zhang YE. Smad-dependent and Smad-independent pathways in TGF-β family signalling. Nature. 2003;425:577–84.